

A STUDY ON THE COLLAPSE LIMIT OF CLT PANEL CONSTRUCTION BASED ON STATIC LATERAL LOADING TESTS

Tatsuya MIYAKE¹, Motoshi SATO², Shoichi NAKASHIMA³, Masahiro MATSUDA⁴, Hiroshi ISODA⁵, Naohito KAWAI⁶

ABSTRACT: There is no example of seismic collapsing behaviour of CLT panel constructions in past earthquakes or shake table tests even in Japan as a high seismic area, leading true collapse limit still unknown. It causes the seismic design standard in Japan probably too conservative. In-plane stiffness and strength of CLT walls are generally larger than the other wooden walls, and the gravitational restoring force from wall rocking is also larger. Therefore, the collapse limit deformation of CLT constructions is expected large. In this paper, based on static lateral loading tests of 2-story models, the lateral load carrying capacity under large deformation, and its causal factors are examined. As results, it is confirmed that the ultimate story drift angle of the test models is 1/4.0-1/3.3rad, indicating the probability of escaping collapse against sever seismic motion. And the restoring force in the region of large deformation mainly depends on tensile resistance of orthogonal walls and moment resistance of lintel-wall connections. These knowledges are useful for optimization of the seismic design standard of CLT panel constructions in the future.

KEYWORDS: CLT panel, Large deformation, ultimate seismic performance, restoring force

1 – INTRODUCTION

Japanese government notification on the structural design of the CLT panel constructions (“GN” in the followings) was issued in 2016. Prior of it, shake table tests of 3 and 5 story CLT panel constructions were carried out in 2014 and 2015 as preparations to establish the rules in GN [1], [2]. However, these test models didn’t collapse leading the collapse limit and seismic collapsing behaviour of CLT panel constructions still unknown. The knowledges on ultimate seismic performance including collapsing behaviour are essential for the optimization of the seismic design standard.

In this study, based on the background above mentioned, firstly, static lateral loading tests of 2-story models are carried out to confirm the lateral load carrying capacity under large deformation. Next, relations of force-deformation of each connection and the causal factors of the restoring force under large deformation are examined based on analyses using simple structural models corresponding the test models. Lastly, on a test model in

the shake table test, the result of time history response analysis using obtained relations of force-deformation of connections is compared with the result of the shake table test to confirm the validity of the force-deformation relations.

2 - STATIC LATERAL LOADING TESTS

2.1 TEST MODELS

Test models were W1, A10N and A10K as shown in Figure 1. Their specifications were as shown in Table 1 and Figure 2, 3 which satisfied GN and JAS (Japanese Agricultural Standard) on the specifications of CLT panels (2013). The compositions of CLT panels were as shown in Fig. 2 where E60 and E30 meant that the lower limit of MOE of laminas was controlled as 6 and 3GPa based on JAS. The species of CLT panel was Japanese cedar. Vertical planes were composed with CLT panels of “S60-3-3” (90mm thickness) connected each other using hardwares shown in Figure 3, screws and bolts. The bottom of the vertical planes is connected to the base frame corresponding foundation similarly with anchor bolts and

¹ Tatsuya MIYAKE, Nihon System Sekkei Architects & Engineers, Tokyo, Japan, miyake@nittem.co.jp

² Motoshi SATO, Nihon System Sekkei Architects & Engineers, Tokyo, Japan, sato@nittem.co.jp

³ Shoichi NAKASHIMA, Dept. of Building Structure, Building Research Institute, Tsukuba, Japan, nkas@kenken.go.jp

⁴ Masahiro MATSUDA, Faculty of Eng., Shinshu University, Nagano, Japan, mat@shinshu-u.ac.jp

⁵ Hiroshi ISODA, Research Institute for Sustainable Humanosphere, Kyoto University, Kyoto, Japan, hisoda@rish.kyoto-u.ac.jp

⁶ Naohito KAWAI, School of Architecture, Kogakuin University, Tokyo, Japan, kawai-nk@nifty.com

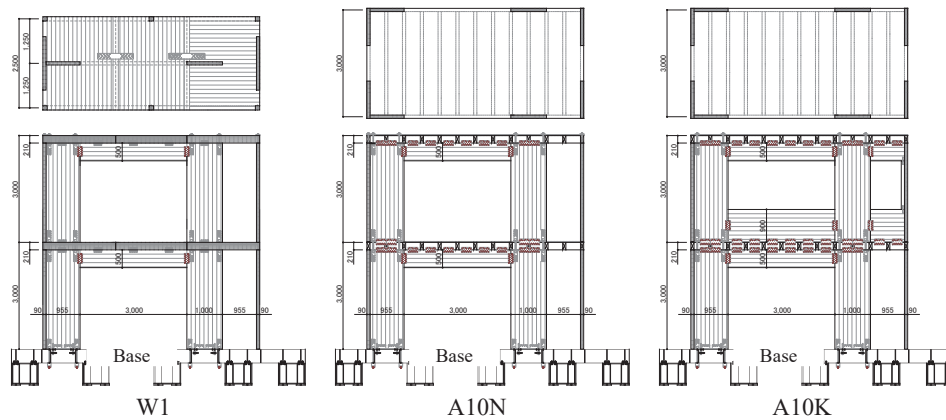


Figure 1. Test models for the static lateral loading tests

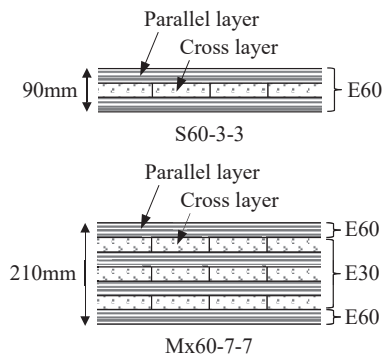


Figure 2. Composition of CLT panel

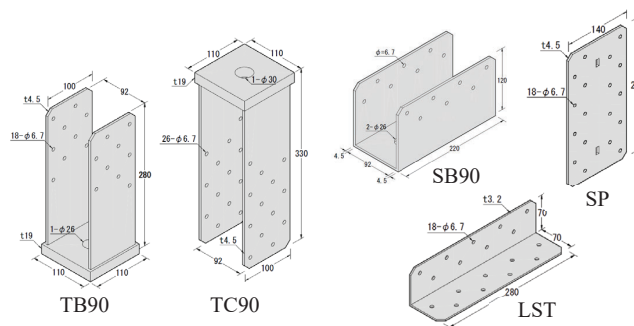


Figure 3. Connection hardware [3]

the shear connector which was newly designed for the test models to keep shear strength under large deformation angle of wall panel. In W1, horizontal planes were composed with CLT panels of “Mx60-7-7” (210mm thickness) connected each other using plywood splines and nails. Horizontal planes in A10N and A10K were

composed with GLT beams and plywood connected each other using hardware or screws. Weights of each model were set as Table 2. For W1, additional weights were set on each floor to make the story weights same as the upper limit ruled in GN. For A10N and A10K, additional weights were set so that story weight per unit floor area was same

Table 1 Specifications of the models

Model	W1	A10N, A10K
Wall	CLT (S60-3-3, $t = 90\text{mm}$) cf. Figure 2	
Floor	CLT (Mx60-7-7, $t = 210\text{mm}$) cf. Figure 2	GLT ($b \times D = 90 \times 210\text{mm}$) + Plywood ($t = 24\text{mm}$)
Tensile connection	Wall-Base; Hardware “TB90” + Screw ($d = 5.5\text{mm}$, $l = 65\text{mm}$) x 18 cf. Figure 3 Bolt ($d = 14.54\text{mm}$, M16, ABR490, JIS B 1220)	
	Wall-Wall, Wall-Roof; Hardware “TC90” + Screw ($d = 5.5\text{mm}$, $l = 65\text{mm}$) x 26 cf. Figure 3 Bolt ($d = 18.20\text{mm}$, M20, ABR490, JIS B 1220)	
Shear connection	Wall-Base; Hardware “SB90” + Screw ($d = 5.5\text{mm}$, $l = 65\text{mm}$) x 18 cf. Figure 3 Flat steel plate ($t = 9\text{mm}$) welded with 2 of SB90 + Steel bar ($d = 24\text{mm}$)	
	Wall-Floor, Roof; Hardware “LST” cf. Figure 3 + Screw ($d = 5.5\text{mm}$, $l = 65\text{mm}$) x 18 cf. Figure 4	Wall-Floor, Roof; Hardware “SP” cf. Figure 3 + Screw ($d = 5.5\text{mm}$, $l = 65\text{mm}$) x 18 cf. Figure 4

Where, t : thickness, b : width, D : depth, d : diameter, l : length

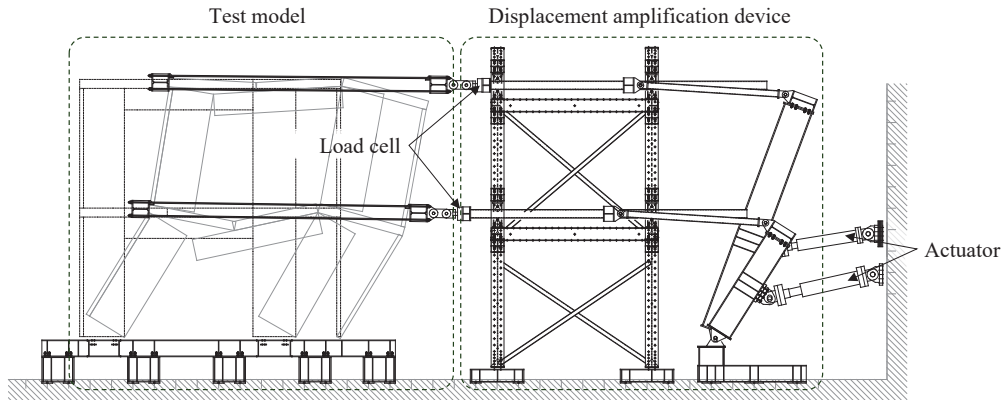


Figure 4. Setting of test apparatus

as W1. Each model was subjected large horizontal deformation corresponding the collapse limit using the loading apparatus shown in Figure 4.

Table 2 Weight of the test models (kN)

Model	W1	A10N	A10K
2 nd story	75.2	85.9	85.9
1 st story	100.6	117.3	121.0
total	175.8	203.2	206.9

2.2 TEST RESULTS

Test models W1, A10N and A10K were subjected horizontal deformation until the restoring force in 1st story became almost zero. In advance, the ratio of story drift of 1st and 2nd story was decided based on the collapsing response analysis assuming the force-deformation relations of connections. And it was modified during the test to keep the ratio of story shear of 1st and 2nd rational.

As test results, envelope relations of story shear and story drift are as shown in Figure 5. Figure 6 shows the relations of acceleration, A and displacement, Δ of the equivalent single degree of freedom system (“ESD” in the followings) obtained as Equation (1) and (2). In Figure 5

and 6, “LOW” means left side orthogonal wall.

$$A = \frac{\sum_i m_i d_i^2}{(\sum_i m_i d_i)^2} Q_B \quad (1)$$

$$\Delta = \frac{\sum_i m_i d_i^2}{\sum_i m_i d_i} \quad (2)$$

where, m_i : mass of i -th story, d_i : relative horizontal displacement from the base of i -th floor level, Q_B : base shear

The provisional collapse limits (“PCL” in the followings) in Figure 5 and 6 are estimated as the point of the maximum displacement or the point where final drop of A begins. States of deformation near PCL are as shown in Figure 7. At PCL, story drift angle in 1st story of W1, A10N and A10K is 1/3.7rad, 1/3.8rad and 1/4.0rad for each, where lateral resistance force survives while all of anchor bolts have fractured. From observation during the test, it was estimated that main lateral resistance element at PCL was in-plane bending force at end of lintels (red circles in Figure 7).

The envelope relation of the acceleration response spectrum S_a and the displacement response spectrum S_d (damping factor, $h = 0.1$) of several past seismic motions of the seismic intensity 7 (the maximum value, Japan

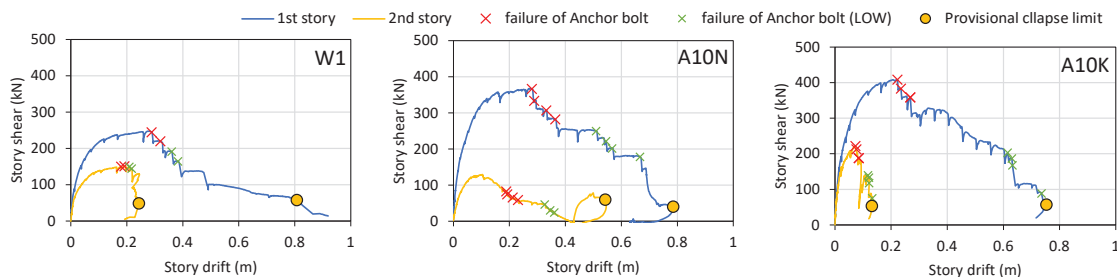


Figure 5. Relations of Story shear – story drift

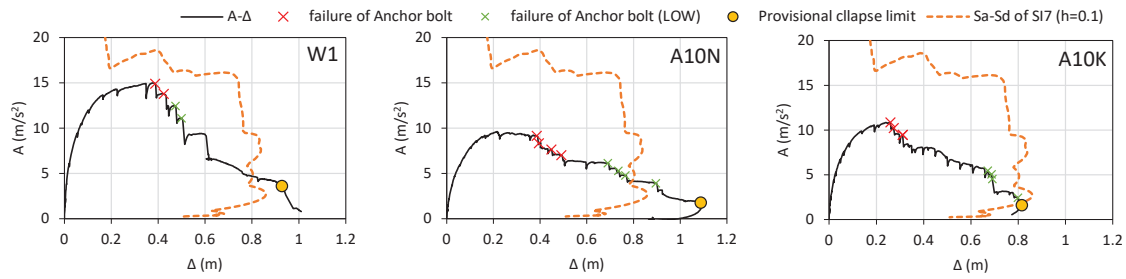


Figure 6. Relations of acceleration – displacement of ESD



Figure 7. States of deformation near the provisional collapse limit

Meteorological Agency, “SI7” in the followings) is inserted in Figure 6 as orange broken line. $A-\Delta$ relation of all test model intersects S_a-S_d relation of SI7 before PCL, indicating the probability of escaping collapse under seismic motion of SI7.

3 – ANALYSES ON THE LATERAL LOAD CARRYING CAPACITY

3.1 STRUCTURAL MODELS

Each test model is assumed as the simple structural model

shown in Figure 8 which has spring elements with nonlinear force-deformation characteristics corresponding each connection. Whole of 2nd story of W1 and A10K is regarded as single shear spring element because its detailed behavior is complicated. In Figure 8, “LOW” means left side orthogonal wall as same as Figure 5 and 6, and “ROW” means right side orthogonal wall.

3.2 METHOD OF ANALYSES

A displacement of each CLT panel in the test is obtained from results of the image measurement as shown in Figure

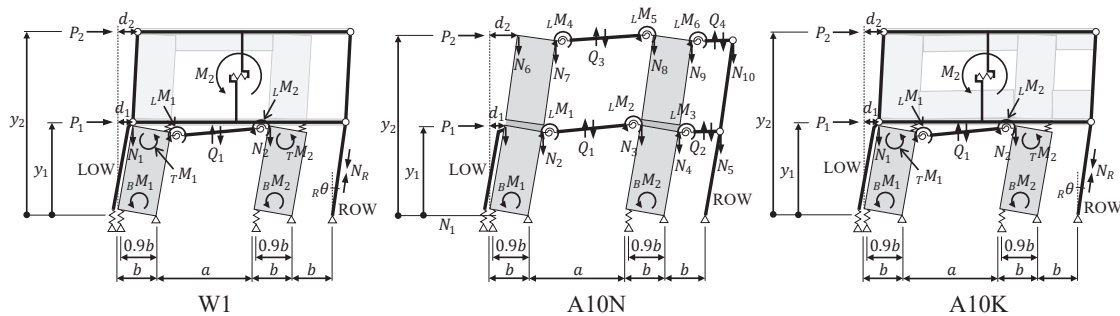


Figure 8. Structural models

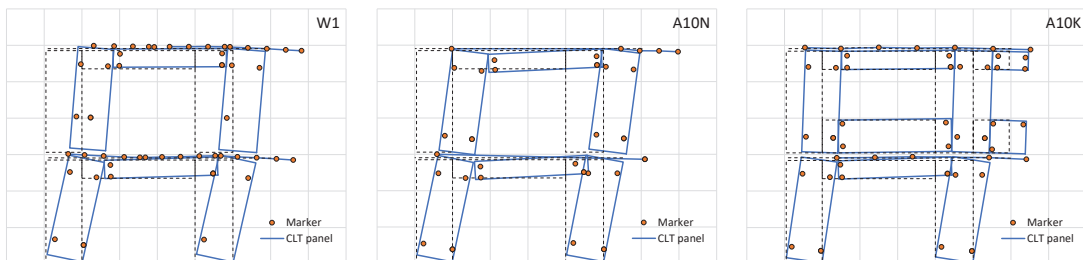


Figure 9. States of deformation from the image measurement (Examples)

9. Using these data and the structural model above mentioned, relation between force, f and deformation, δ of in-plane bending of lintel and wall connections which is the unknown factor, is analyzed according to steps below.

Step 1: Deformation, δ of each connection, neural axis, x_n at top and bottom of wall panels, height of lateral load, y_1, y_2 , and relations between them and story drift, δ_{si} are obtained from displacement of CLT wall panels. Then approximate functions of δ_{si} corresponding to these relations are obtain as shown in Figure 10.

Step 2: Relation of force, f and deformation, δ of each connection is assumed.

Step 3: δ_{si} measured in the test is applied to the function obtained in Step 1 to calculate δ, x_n, y_1, y_2 .

Step 4: δ is applied to relation assumed in Step 2 to obtain f .

Step 5: Moment of 2nd story, M_2 and of ROW, M_{ow} are calculated as Equation (1) and (2). Bending force of each member is calculated from f and x_n , which are added up for each member kind as Equation (3) to (5). All of them are summed to obtain structural resistant moment, M_5 .

$$2^{nd} \text{ Story} \quad M_2 = P_2(y_2 - y_1) \quad (1)$$

$$\text{Orthogonal wall (ROW)} \quad M_{ow} = y_1 N_R \tan_R \theta \quad (2)$$

$$\text{Wall bottom} \quad M_b = \sum_i^B M_i \quad (3)$$

$$\text{Wall top} \quad M_t = \sum_i^T M_i \quad (4)$$

$$\text{Lintel} \quad M_l = \sum_i^L M_i \quad (5)$$

Step 6: Resistant moment from gravitational restoring force due to wall rocking, M_W is calculated based on displacement of CLT wall panels, vertical load, N_i and vertical shear force of lintel, Q_i .

Step 7: overturning moment, M_p from lateral load, P_1, P_2 is calculated as Equation (6).

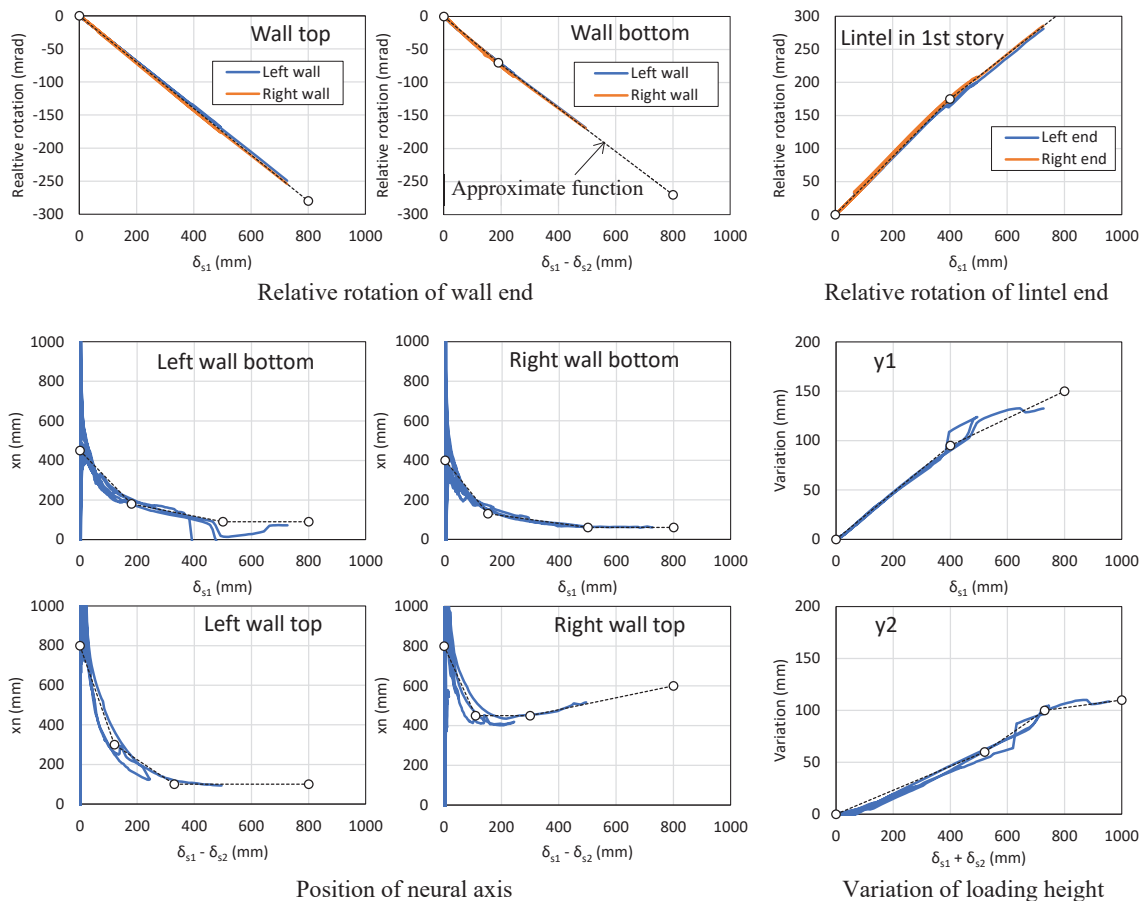


Figure 10. Rotation of wall end, position of neural axis and variation of loading height from image measurement (of W1 as Example)

$$M_p = P_1 y_1 + P_2 y_2 \quad (6)$$

Step 8: If sum of M_S and M_W doesn't agree with M_p , f - δ relations are modified mainly on lintel-wall connections, then return to Step 4.

3.3 RESULTS OF ANALYSES

Force-deformation relation of each connection is obtained through the repeat of modification and calculation according to Step 4-8 mentioned before. Though main objects of modification were lintel end connections, tensile connections were also modified slightly from initial relations which were set based on the specification of bolts to improve agreement to the test results. Besides, tensile resistances of shear connections of wall tops of W1, A10K and lintel ends were also considered from same reason.

As result, the relations are set as shown in Figure 11. Difference of relations of tensile connections among test models which have same specification, is small enough to regard rational. The relations of lintel ends are different considerably for each test model. About A10N and A10K, the relation should be same because the specifications of lintel end connection and floor are same. This difference indicates possibility that the relation of A10N is overestimated. Its reason is guessed that moment resistances of wall top in 1st story and wall bottom in 2nd story are assumed zero.

Figure 12 shows relation between resistant moment and 1st story drift, δ_{s1} calculated based on the relations shown in Figure 11. Total resistant moment, $M_S + M_W$ well agrees with test result, M_p for all test models. About W1, M_b and M_t disappear when δ_{s1} reaches around the range from

0.4m to 0.6m. M_t keeps strength until δ_{s1} reaches around 0.7m. Main resistant element at PCL is M_{ow} . Under large deformation, the axial force of ROW, N_R becomes tensile because of floor rising by rocking of wall panels. About A10N, M_b disappears when δ_{s1} reaches around 0.6m. Resistant element at PCL is only M_t . However, the contribution of moment resistance of lintel ends is possibly overestimated as mentioned above. About A10K, M_b and M_t disappear when δ_{s1} reaches each around 0.6m and 0.4m. Main resistant elements at PCL are M_t and M_{ow} .

4 – APPLICATION TO A SHAKE TABLE TEST

As mentioned before, shake table tests of 3 and 5 story CLT panel constructions were carried out in 2014 and 2015 [1], [2]. One of the test models, model E shown in Figure 13 had almost same specifications with W1. Model E is converted into 3-dimensional structural model with nonlinear spring elements corresponding to each connection to execute time history response analysis. The force-deformation relations of the spring elements are set based on the relations of W1 shown in Figure 11. Model E was excited several times prior of the final excitation by

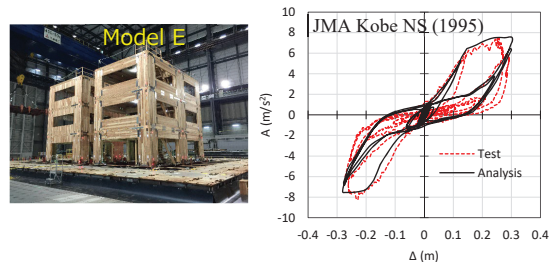


Figure 13. Test model and result of a past shake table test

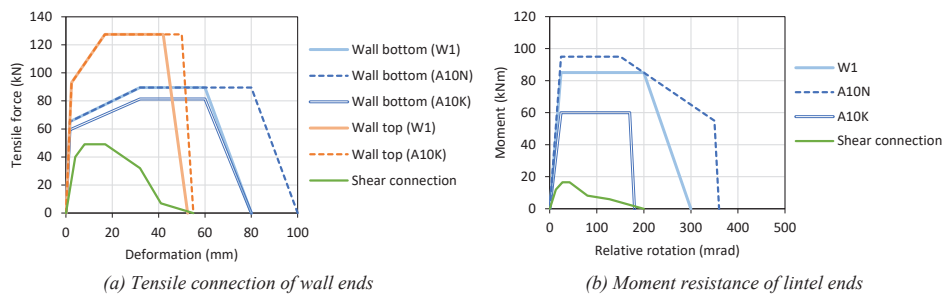


Figure 11. Force-deformation relations of connections

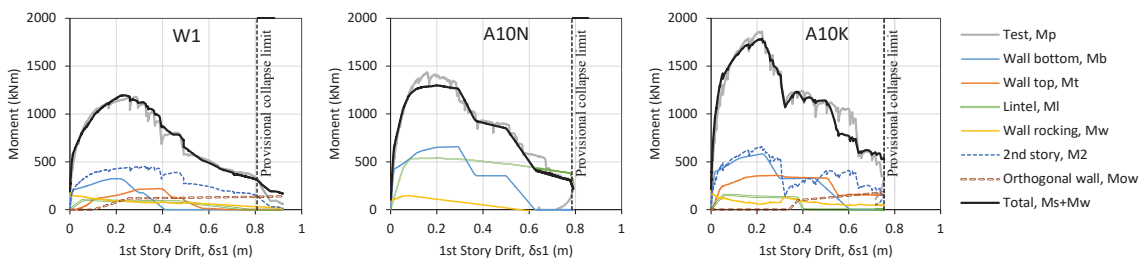


Figure 12. Comparison of analyses and test result, resistant moment apportionment of each element

JMA Kobe NS (1995) in the test. In the analysis, these seismic motions are input sequentially as same as the test. As the result of the analysis, the relation of acceleration, A and displacement, Δ of ESD in the final excitation is as Figure 13. That well agrees with the test result, indicating appropriateness of the relations of $W1$ shown in Figure 11, at least in the deformation range of the shake table test.

4 – CONCLUSIONS

Based on the static lateral loading tests of 2-story CLT constructions, it was confirmed that the ultimate story drift angle was enough large to confirm the probability of escaping collapse against sever seismic motion. Then the force-deformation relations of each connection were estimated to examine the causal factors of restoring force from the analyses using the simple structural models. Lastly, the time history response analysis corresponding to a past shake table test was executed to confirm that the force-deformation relations of connections are appropriate.

The knowledge obtained here is useful for optimization of the seismic design standard of CLT panel constructions in the future.

7 – REFERENCES

[1] N. Kawai, T. Miyake, M. Yasumura, H. Isoda, M. Koshihara, S. Nakajima, Y. Araki, T. Nakagawa and M. Sato. “Full scale shake table tests on five story and three story CLT building structures” In: Proceedings of WCTE, Vienna, Austria (2016)

[2] M. Sato, N. Kawai, T. Miyake, M. Yasumura, H. isoda, M. Koshihara, S. Nakajima, Y. Araki and T. Nakagawa. “Structural design of five-story and three-story specimen of the shaking table test” In: Proceedings of WCTE, Vienna, Austria (2016)

[3] Japan Housing and Wood Technology Center. “Cross-Mark hardware for the connections of CLT panel constructions” (2019), (in Japanese)

ACKNOWLEDGEMENT

This study was carried out as the research project subsidized by the Forestry Agency of Japan. The authors would like to express gratitude to whom it may concern.